JOURNAL OF MATERIALS SCIENCE 32 (1997) 2291–2303

The compressive deformation of cross-linkable PPXTA fibres

M.-C. G. JONES*, D. C. MARTIN‡
Materials Science and Engineering and the Macromolecular Science and Engineering Center, 2022 H.H. Dow Building, Ann Arbor, MI 48109, USA

A study has been conducted on the compressive deformation behaviour of thermally cross-linkable poly(*p*-1,2-dihydrocyclobuta phenylene terephthalamide) (PPXTA) fibres. The morphology of the failure zones was examined by scanning electron microscopy and dark-field transmission electron microscopy. On increasing the heat-treatment temperature from 260–400 °C, and therefore with increasing cross-link density, fewer kinks per unit length were displayed after compressive deformation. The kink specific energy was estimated to increase by a factor of 30, as determined by quantitative measurements of kink density at a given strain and of the critical strain to kink formation. Thus, the intermolecular cross-links still allowed deformation to proceed by kinking, but significantly raised the energy of kink formation. Finally, rupture zones were predominantly observed in axially compressed PPXTA fibres heat-treated at 440 °C. Compressive failure of the fibres changed from kink-dominated failure to brittle rupture with increased heat-treatment temperature, evidently as the result of cross-linking or of chain degradation. A dislocation model of the kink boundary developed by Vladimirov *et al.* was analysed and critically compared with our data. The analysis of this theory with our experimental results suggested that the dramatic change in compressive behaviour with cross-linking was due to a transition from fine intermolecular shear to blocky interfibrillar shear.

1. Introduction

Yielding generally limits the use of polymer materials for structural applications, but at the same time provides for toughness and prevents brittle fracture. Oriented polymers often yield in compression by the formation of kink bands. A kink band is a localized region of plastic shear deformation where the molecules have undergone a large change in orientation. The sheared region is separated from the undeformed part of the sample by a high-angle boundary on each side. Thus the formation of a kink band involves local intermolecular or interfibrillar slippage as well as bending or buckling of the polymer chains at the boundaries. Because the formation of kink bands precedes compressive failure, an understanding of how the kinking process depends on the morphology should make it possible to optimize structures for higher compressive strength.

The compressive deformation behaviour of cross-linkable poly(*p*-1,2-dihydrocyclobuta phenylene terephthalamide) (PPXTA) extended-chain fibres has been studied in this work. The rationale for designing a cross-linkable PPXTA fibre was to restrict the intermolecular shearing observed within kink bands, and therefore to raise the energy and stress to kink formation [1, 2]. The morphology of the yielding and fracture areas including kink bands was investigated in the axially compressed PPXTA fibres of various intermolecular cross-link densities. Numerical estimates of kink linear density were obtained to quantify the energy involved in creating kink bands in uncross-linked and cross-linked materials. We compare our experimental results to numerical calculations predicted by the Vladimirov model [9] for the uncross-linked and cross-linked PPXTA. The implications of our results are reviewed.

Experimental results and theories on the kink band formation in diverse materials such as metals, mineral crystals, composites, carbon fibres and oriented polymers, have been surveyed in a number of articles [1–5]. We review a few major studies of the compressive behaviour of extended-chain polymers.

DeTeresa *et al.* [6] postulated that the compressive failure in anisotropic organic fibres results from the local elastic microbuckling of polymer chains preceding the collapse into a propagating kink band. An analysis of the buckling of a collection of oriented and laterally-interacting extended polymer chains

* *Present address:* Union Carbide Corporation, P.O. Box 670, Bound Brook, NJ 08805, U.S.A.
‡ Author to whom all correspondence should be addressed.

0022–2461

predicted a compressive strength or critical stress equal to the longitudinal shear modulus, e.g. $\sigma_{comp} = -G$ where G is the minimum longitudinal shear modulus. The compressive strength was estimated as the product of the strain to kink formation and the tensile modulus. A linear relationship was found between the axial compressive strength, σ_c, and the shear modulus, G, for various liquid crystalline fibres and graphite fibres, supporting the concept of compressive failure due to molecular elastic microbuckling instability. It was pointed out that the relevant longitudinal shear modulus is the minimum longitudinal shear modulus which, in the case of the radially organized Kevlar, corresponds to the torsional modulus or $G_{\theta Z}$. The compressive strengths were found to be approximately one-third of the torsional moduli owing to, according to the authors, residual stresses and misalignment of polymer chains.

Martin [1] and Martin and Thomas [2] studied kink band morphology in compressed PBZO and PBZT using transmission electron microscopy (TEM). TEM dark-field imaging showed that the material within the kink bands was misoriented but remained laterally ordered. High-resolution electron microscopy (HREM) revealed the non-uniformity of the strain within the kink bands. The shear within the kink band was described as blocky rather than fine. Different features for the boundaries on each side of the kink bands were typically observed with dark-field TEM imaging. The boundary in the tensile region of the kink band (where the local deformation is away from the centre of the fibre) was sharper than the boundary in the compressive region of the kink band. Martin and Thomas proposed a model of a kink band, adapted from a twin dislocation model [7], containing tilt boundaries and partial dislocations of burgers vector parallel to the kink boundary, or perpendicular to the chain axis direction. This dislocation model was used to estimate the form of the stress field around the kink band. Using the approximation of linear isotropic elasticity, the narrow and broad kink boundaries were estimated to be in a state of hydrostatic tension and compression, respectively. A schematic illustration of the regions of hydrostatic tension and compression near the front of a propagating kink is shown in Fig. 1.

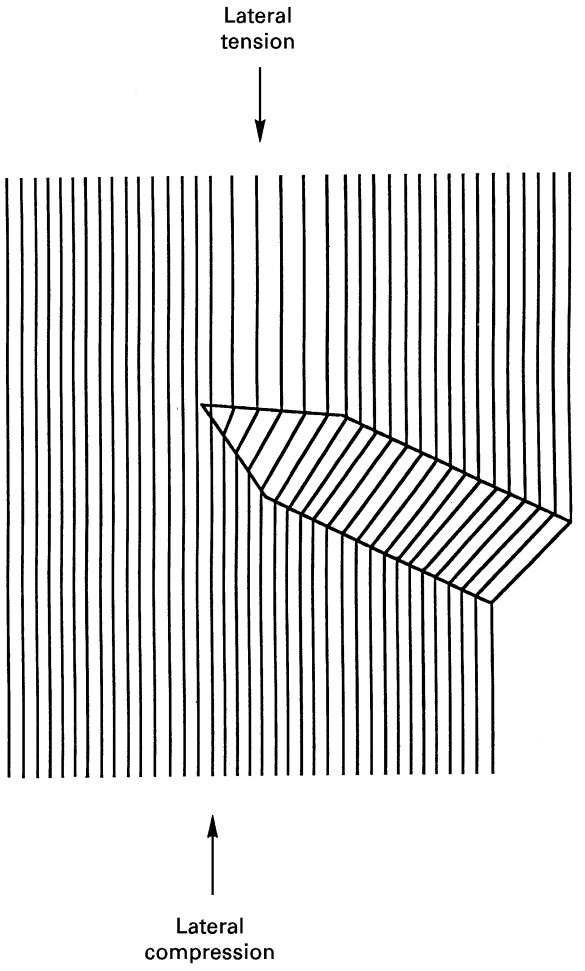

Figure 1 Schematic drawing of a propagating kink band showing regions of local tension and compression in the vicinity of the zone of sheared material.

Lee and Santosh [8] argued that the fibrillar structure is primarily responsible for the low compressive strength of rigid-rod polymeric fibres and that, in general, the fibre can deform in three buckling modes: the buckling of a homogeneous fibre, the buckling of a collection of interacting fibrils, and the buckling of a collection of non-interacting fibrils. The actual buckling mode corresponding to the lowest critical buckling load value is governed by the aspect ratio of the buckling units or fibrils and by the degree of interaction between them, e.g. by the interfibrillar shear modulus, G, and transverse modulus, E_t. Given the assumption of a buckling instability, it was demonstrated that a fibre with an internal structure (imperfect glue) will have an instability at a lower compressive stress compared with a fibre without the internal structure (perfect glue). It was pointed out that the distribution of the values of E_t and G and of the aspect ratio of the buckling elements within the fibre may lead to the instability being initiated in different modes at different regions in the fibre. For PBZT the instability of the fibrils was predicted to occur in the shear mode. In addition, for a fibril length to diameter aspect ratio, l/d, greater than 100, the critical buckling stress in the shear mode was approximated by the shear modulus, G, and was independent of the tensile modulus. The interfibrillar shear modulus, G, would correspond to the torsional modulus. However, the choice of the value of l/d, and more specifically of l, for the fibrils and microfibrils, is debatable. By examining scanning electron micrographs of kink bundles, the parameter l was approximated as the original length along the fibre that comprises the kink region, roughly 1–100 μm. However, the SEM image represents a bundle of kinks, and kinks as small as 30–50 nm have been observed [2] making the l/d ratio much smaller than 100.

Vezie [5] presented a microstructural analysis of the kink structure and geometry in PBZO fibres, based on low-voltage SEM analyses. Sharp or diffuse kink band boundaries were observed, but not necessarily on the tensile and compressive region of the

kink bands. A proposed model of a kink band containing edge dislocations of Burgers vector parallel to the chain axis direction, was adapted from previous models [9, 10]. Arguments were presented supporting the concept that shear instability causes kink initiation in PBZO fibres. Unlike the microbuckling models which consider that a fibre has a perfectly aligned structure, the shear instability model [11, 12] takes into account structural imperfections such as crystallite or fibril misorientation. Compressive failure is initiated by local shear failure when a resolved shear stress on the slip plane of a slightly misoriented region, parallel to the compression axis, reaches the shear strength. The stress to initiate shear slip is $\sigma_{comp} = -\tau/\varphi_0$ where τ is the shear strength corresponding to the slip system, and φ_0 is the misalignment angle between the slip direction on the slip plane and the compression axis. Observations of kink bands in PBZO showed that the angles α and β follow the relation $\beta \geq \alpha/2$ and therefore that the material within the kink bands is typically in tension [5]. α and β represent the kink inclination, determined by molecular rotation or fibre rotation for a fibre composite, and the boundary inclination, respectively [13]. The volumetric strain consists of a uniaxial strain, ξ, and is given by $\xi = \cos(\beta - \alpha)/\cos(\beta) - 1$. The minimum strain energy in the kinked zone corresponds to an angle β of $\beta = \alpha/2$ [13].

Pertsev *et al.* have developed theories for the nucleation, propagation, structure and movement of kink bands in oriented polymers [9, 14–18]. Their work emphasizes the role of defects on oriented polymer's plastic deformation, failure, and behaviour during processing [19]. The models were developed to explain the nucleation and propagation of microscopic kink bands, the width of whose boundaries is of the order of the interatomic distance. As pointed out by the authors, they are not adequate to describe the structure of macroscopic kink bands characterized by boundaries with significant width.

Vladimirov *et al.* [9] proposed a dislocation model of a boundary of a macroscopic kink band and developed a theory which enables calculation of the most important parameters of the boundaries: their width and specific energy. We have analysed this model in detail because developed kink bands of macroscopic size are usually observed in microscopes, and because the two quantities that can be calculated may be obtained experimentally. In this model it is assumed that the kink bands are formed primarily by microfibril slipping, and that intrafibrillar shear is negligible. An elementary disorientation boundary of microfibrils is modelled by a wall of dislocations of Burgers vector parallel to the chain axis, separated by a distance equal to the size d of the microfibrils or bending elements. The model of the boundary consists of some number of dislocation walls aligned parallel to one another. The width, L, of the boundary of the kink band is determined by the condition that the total specific energy, W, of the boundary is minimum. The contributions to W are the characteristic energies of dislocation walls, the energies of their elastic interaction, and the energies resulting from the transverse tensile strain. The model is presented in more detail in Section 3.

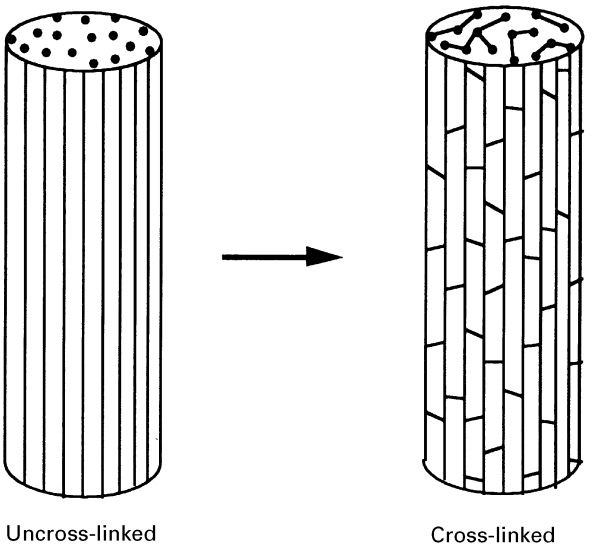

Figure 2 Schematic drawing of oriented, extended-chain polymer fibres before and after cross-linking.

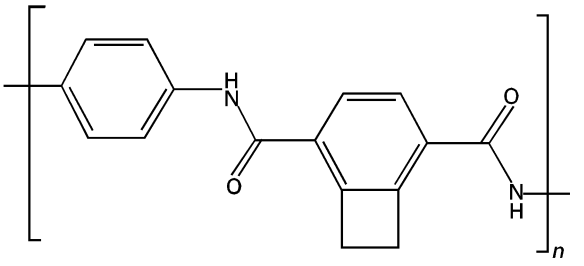

Figure 3 Chemical structure of the PPXTA polymer.

Thus the instability leading to the formation of a kink band has been explained differently by two major mechanisms: the buckling of fibrils or molecules, and the shear instability. In both cases, the stress to initiate the instability was assumed to be the critical stress to kink formation. Furthermore, the kinking and the compressive strength were assumed to coincide. For both instability mechanisms, the critical length scale was not well established. Buckling could be at the molecular, fibrillar, or other level. Similarly, shear could be fine or coarse, for example intermolecular or interfibrillar.

PPXTA is a cross-linkable version of PPTA and was developed to modify the macroscopic properties of PPTA, including its deformation behaviour in compression. The role of the intermolecular cross-links on the two micromechanisms of deformation that may operate during kinking, buckling or shearing, is studied here. This will make it possible to establish the local nature of the deformation during axial compression of oriented fibres in general.

Fig. 2 shows schematically the structure of normal extended-chain fibres compared with cross-linked extended-chain fibres. PPXTA polymer is synthesized from the XTA monomer instead of the conventional terephthalic acid (TA) used for PPTA [20, 21]. A schematic representation of PPXTA is displayed in Fig. 3.

The benzocyclobutene (BCB) moiety is a thermally activated cross-linking group, that reacts by opening of the cyclobutene ring at temperatures above the synthesis and spinning temperatures but below the polymer degradation temperature. Thus PPXTA may be cross-linked in the solid state during a post-spinning heat treatment. Cross-linking in the solid state after shape forming makes it possible to retain the high degree of orientation and order that characterizes these high-performance fibres and results in their excellent tensile properties.

The processing, microstructure, and properties of cross-linkable PPXTA fibres have been described elsewhere [22, 23]. Differential scanning calorimetry experiments revealed that the exothermic cross-linking reaction starts at 300 °C and is completed at about 425 °C. Thus one may compare uncross-linked materials, heat treated below 300 °C, to cross-linked materials heat treated above 300 °C. The higher the heat-treatment temperature and time, the greater is the density of intermolecular crosslinks. This increase in cross-link density is coupled with an improvement in orientation and degree of crystallinity.

Lyotropic liquid crystalline polymers such as PPTA and PPXTA are known to form a microfibrillar network during coagulation of the oriented lyotropic solution in a non-solvent bath (water) [24, 25]. The crystalline structure of PPXTA is similar to that of PPTA, with the molecules being hydrogen bonded, and the distance between hydrogen-bonded planes being greater in the case of PPXTA. The X-ray diffraction patterns of uncrosslinked and crosslinked fibres appeared similar, suggesting that most of the cross-links preferentially form in the grain-boundary phase between crystallites. Furthermore, the cross-linking reaction may be restricted within the microfibrils. The experimental nuclear magnetic resonance and Fourier transform–infrared evidence to date has been consistent with a carbon–carbon double bond between aromatic rings as the predominant mechanism of BCB cross-linking [26, 27]. This is in agreement with the suggestions of Marks [28, 29] on the possible products of BCB homopolymerization. A free-radical mediated thermal degradation process was thought to take place concurrent with cross-linking during the heat treatment, and is probably responsible for the observed loss of tensile strength at the highest heat-treatment temperatures [30].

2. Experimental procedures

As-spun PPXTA fibres synthesized at the University of Michigan and spun at DuPont were heat treated under 0.3 GPa tension, in a nitrogen atmosphere, for 30–120 s, at intermediate temperatures (260 °C) to increase crystallinity and orientation, and at higher temperatures (415–440 °C) to trigger the BCB cross-linking reaction. The degree of cross-linking varies with the heat-treatment conditions.

The method used to apply a small and uniform compressive strain to the fibres was by shrinkage of a surrounding polymer matrix [31]. The technique involves casting a solution of 10 wt % nylon-6,6 in formic acid over the fibre on a glass slide. With solvent evaporation, the nylon film shrinks as it densifies, putting the fibre in compression. Owing to the adhesion of the nylon film to the glass slide, most of the film shrinkage occurs after it is peeled off the plate. The magnitude of the compressive strain was approximately 3%.

The morphological features of kinks and other localized failure zones obtained with this technique were observed with a Hitachi 800 SEM and a JEOL 4000 TEM. For SEM observation, the samples were lightly coated (15 s) with gold and palladium and the operating voltage was 2 V [32]. The number of kinks and kink bundles were counted over a fibre length ranging from 3.5–5 mm, while visualizing the fibre sample in the SEM at a magnification of $\times 1000$ and an appropriate scan speed for best resolution. A linear density of kinks and kink bundles (kinks/mm) was thereby obtained. For TEM observation, the samples were microtomed to a nominal thickness less than 0.1 μm, and deposited on a copper grid coated with a thin carbon layer. The operating voltage was 400 kV and the dose of electrons received by the sample never exceeded $0.1 C\,cm^{-2}$ to preserve the crystallinity and integrity of the material [33].

The beam-bending method [34] was used to determine the critical strain to failure associated with the visualization of kink bands or bundles of kink bands. This technique involves bonding the fibre with an acrylic spray to a clear polycarbonate elastic beam and loading the beam in cantilever bending. A known compressive strain distribution which varies linearly along the length of the beam can be calculated from elasticity theory. Yielding, corresponding to the formation of kink bands visible with optical microscopy, makes it possible to calculate a critical strain to kink formation. The polycarbonate bar and acrylic film may be assumed to behave elastically up to 1% [34].

The dislocation model of a kink band boundary developed by Vladimirov *et al.* [9] was analysed with a FORTRAN program. The theoretical stiffness constants or moduli for uncross-linked and cross-linked PPXTA and PPDXTA crystals were obtained from molecular simulations using the CERIUS software package and the Dreiding II force field [35]. PPDXTA contains twice as many cross-links as PPXTA because the diamine moiety is a benzodicyclobutene [36]. The theoretically predicted change in the elastic constants of crystalline PPDXTA upon cross-linking was used to analyse the Vladimirov model.

3. Results and discussion

The compressed PPXTA fibres were observed with optical microscopy and SEM to detect any major change in their kinking behaviour after cross-linking. Representative SEM images of kinks or failure areas in PPXTA as-spun, heat treated at 260 °C for 1 min, at 418 °C for 1 min, at 435 °C for 2 min, and compressed with the nylon matrix shrinkage technique, are

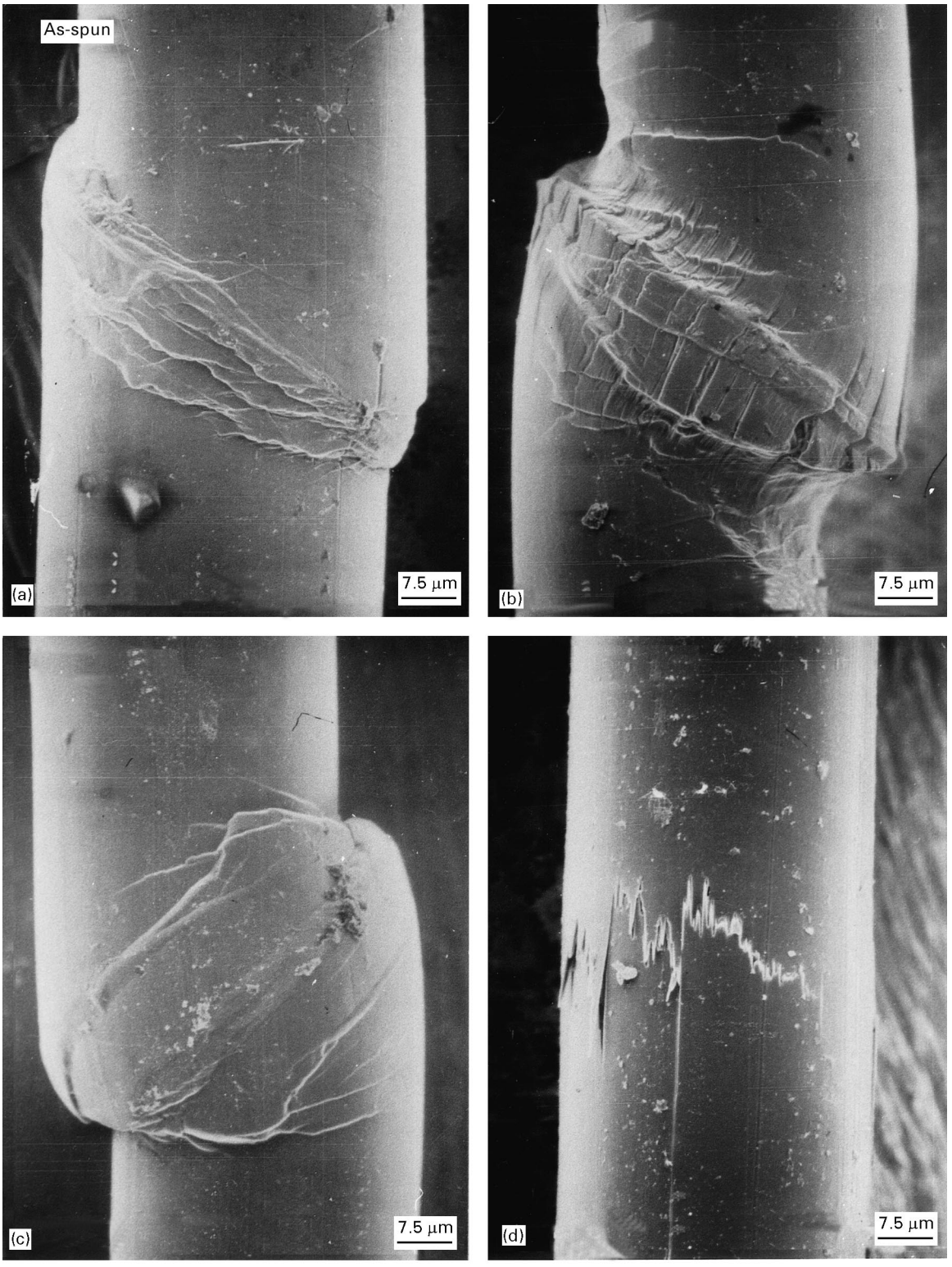

Figure 4 SEM images of kinks or failure areas in PPXTA (a) as-spun and heat treated for various temperatures and times: (b) 260 °C for 1 min, (c) 418 °C for 1 min, and (d) 435 °C for 2 min.

displayed in Fig. 4. Whereas some kinks and kink bundles were observed on the fibres heat treated up to 418 °C for 1 min and even on the fibres heat treated at 435 °C for 1 min, only features involving some material fracture and small kinks barely detectable with SEM were observed on the fibres heat treated at 435 °C for 2 min. The local fracture areas involve some rupture of the microfibrils and of the molecular chains, and may result from a brittle behaviour because no yielding, such as the formation of kink bands, was observed preceding their formation. A few brittle fracture features were also observed in the fibres heat treated at 418 for 1 min, in addition to kink bands. The fibres heat treated at 435 °C for 2 min were broken at several areas during compression in the nylon matrix. Thus by increasing the heat-treatment temperature or time, a transition in compressive failure behaviour is observed from kinking to brittle

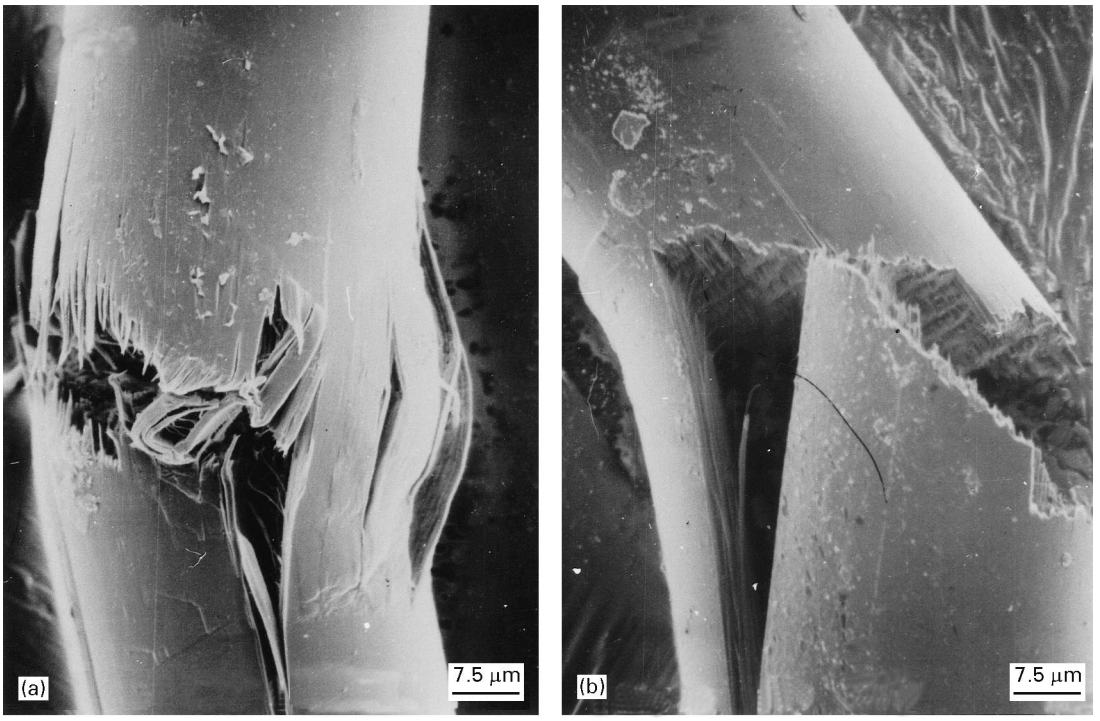

Figure 5 SEM images of the failure area in PPXTA heat treated at (a) 418 °C for 1 min and (b) 435 °C for 2 min.

rupture. This is strikingly different from the behaviour of commercial PPTA (Kevlar 49) which exhibits a very high density of kink bands after compression in a nylon matrix, before or after a heat-treatment at 435 °C for 2 min.

Differences in the morphology of the kink bands in fibres heat-treated at 260 °C for 1 min and at 418 °C for 1 min may be seen in Fig. 4 and were seen on other kinks observed via the SEM. Numerous cracks on the kink bundles running parallel to the fibre axis are exhibited by the uncross-linked fibres heat treated under tension, and not by the cross-linked fibres. Longitudinal cracks have been observed before in Kevlar 49 [37, 38]. It has been suggested that the presence of microcracks may indicate that the degree of shearing between adjacent molecular chains is non-uniform [37, 38]. Microcracks may also result from a transverse strain in the kink band $\xi = (\delta - \delta_0)/\delta_0$ where δ is the thickness of the strained shearing elements, and δ_0 is the original thickness of the shearing element [9, 13]. Typically band boundaries are asymmetric in a manner that leads to an increased volume within the kink band [5]. Thus ξ is a tensile strain which increases with bending. At some point, ξ exceeds the transverse yield and an interfibrillar crack appears. Vladimirov *et al.* [9] have pointed out that the transverse strain rapidly increases with growing kink angle and that interfibrillar stratification starts at a critical angle. Cracks from different kinks within a kink bundle merge. Our results on the lateral compressive deformation behaviour of PPXTA fibres show that the transverse yield stress is higher for the cross-linked fibres. A higher transverse yield stress would explain why large cracks are less common in cross-linked materials. The lack of cracks also suggests that the overall lateral connections in the cross-linked fibres are stronger, thus the individual fibrils are not so well defined. Also, no cracks were observed in the as-spun fibres or in fibres heat treated without tension, presumably because less-oriented fibres do not provide for an easy path for crack propagation.

A typical failure area obtained during compression in the nylon matrix is shown in Fig. 5 for PPXTA heat treated under tension at 418 °C for 1 min and at 435 °C for 2 min. The failure is mostly observed on the tensile side of the bent fibres. The fibres heat treated at 418 °C display a fibrillar fracture surface whereas the fibres heat treated at 435 °C display a less fibrillar fracture surface, where the periodicity of the surface features may be related to the pleated structure. A similar morphological transition was observed previously on the tensile fracture surfaces of mildly heat-treated and cross-linked fibres [22]. This transition was attributed to degradative chain scission. This transition may also indicate an increased connectivity between the fibrils due to some interfibrillar crosslinks. This was found to be the case for cross-linked polyethylene fibres, where a similar morphological transition was not accompanied by a loss of tensile strength [34].

At least three different phenomena take place during heat treatment: improved orientation and crystallinity [23], cross-linking [22], and a possible chain-degradation process associated with the BCB chemistry [30]. To limit the effect of possible chain degradation, the fibres were kinked with the nylon matrix shrinkage technique a few hours after they were heat treated. In the event, however, that thermal degradation occurred significantly, the question remains of the behaviour that would be exhibited by a hypothetical cross-linked and not degraded fibres. One possibility would be that no material fracture would be observed in the fibres heat treated at 435 °C

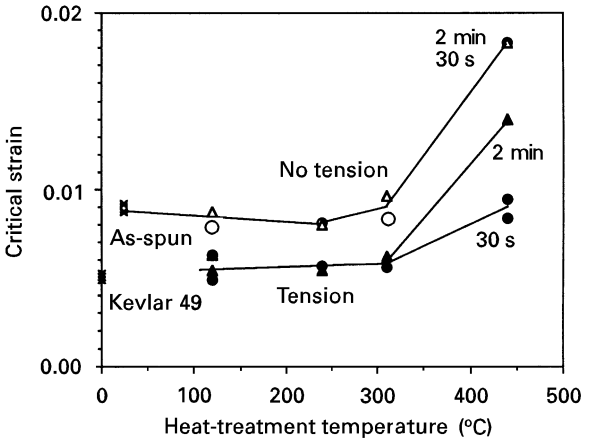

Figure 6 Critical strains to kinking for PPXTA fibres as a function of heat treatment. The strain to kinking for Kevlar 49 is also shown.

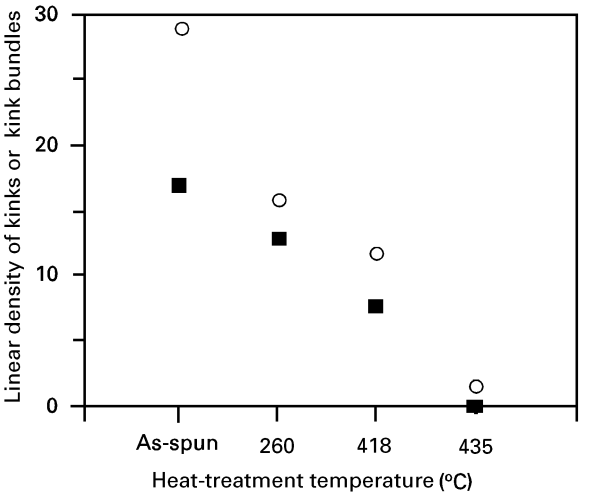

Figure 7 Linear density of (○) kinks and (■) kink bundles as a function of heat-treatment temperature. The heat-treatment time was 1 min.

for 2 min as a result of the applied 3% strain, and therefore that no yielding and no signs of failure would be exhibited at this strain. It is also possible that significant axial cracking would be observed in the kink bundles of the fibres heat treated at 418 °C for 1 min. The explanation would be that the plastic deformation could not be accommodated without a large amount of chain ends created by thermal degradation, resulting in crack formation.

Fig. 6 shows the critical strain to compressive failure or kink formation, ξ_c, as a function of heat treatment using the beam-bending method. The uncross-linked fibres heat treated below 310 °C kink at approximately the same strain regardless of the heat-treatment temperature and time. This indicates that increasing crystallinity and orientation does not significantly change the onset of kinking. The as-spun fibres and fibres heat treated under no tension appear to kink at a higher strain. This appears to be related to the fact that it is difficult to visualize kinks in a pleated structure, which is more pronounced if no tension is applied to unfold the pleats. Martin and Thomas [2] found no major difference in the critical strain to kink formation for as-spun and heat-treated PBZO fibres. In contrast, Young [40] found that the compressive strain of poly(2,5(6)-benzoxazole) (ABPBO) was higher for as-spun fibres than for heat-treated fibres. It should be noted that the absolute values of strains above 1% are to be taken with caution as outlined in Section 2. Raising the temperature of the 30 s heat treatment to 440 °C and therefore inducing intermolecular cross-linking, results in a 60% increase in the critical strain to kink formation from 0.55% to 0.9%. From the values of the critical strain to failure, and if the compressive elastic modulus is known, the critical stress to failure can be estimated. However, the compressive elastic modulus is typically lower than the tensile modulus, 55% lower in the case of Kevlar 49 [41]. The difference observed between the fibres heat treated at 440 °C for 30 or for 120 s suggests that more cross-linking takes place with longer time at 440 °C. We emphasize that only one or two failure zones were detected on the fibres heat treated at 440 °C for 120 s strained to 1.4%, and that these failure zones may have been fracture areas.

Together with an increase in critical strain to failure with cross-linking, a severe decrease in linear kink density is observed. Thus the formation of crosslinks in PPXTA fibres not only raises the strain to kink formation but also decreases the density of kinks obtained at a given strain. Fig. 7 displays the kink densities obtained from SEM observation for fibres heat treated for 1 min at various temperatures. Only two or three single kinks per millimetre were observed in the fibres heat treated at 435 °C for 1 min. Significantly fewer kinks were observed in the fibres heat treated at 435 °C for 2 min, at most three over a length of 5 mm. As stated earlier, fibres heat treated at 435 °C for 2 min were broken at several areas during the 3% compression in the nylon matrix. Thus 3% is above the critical strain for brittle rupture of the highly cross-linked fibres.

Martin [1] and Martin and Thomas [42] showed that the specific energy of formation of a kink is related to the critical strain to failure and to the linear density of kinks through the compressive axial strength and the average surface area of a kink boundary. We review here the calculations that make it possible to estimate the energy penalty for the formation of a kink in a uncross-linked and in a cross-linked fibre, heat treated, respectively, at 260 and 435 °C for 1 min.

The plastic strain, ξ_p, associated with the formation of kinks is $\xi_p = \xi_{total} - \xi_{yield}$ with ξ_{total} the total strain imposed by the shrinkage of the nylon matrix, and ξ_{yield} the strain at yield or critical strain to kink formation. Assuming ideal plasticity, the total excess energy of the kinks, E_{total}, is $E_{total} = \sigma_{yield}\xi_p V$ with σ_{yield} the critical stress to kink formation and V the fibre volume. The volume is equal to the area of the cross-section, A_0 times the length of the fibre, l or $V = A_0 l$. The energy per kink is $E_{kink} = E_{total}/N$ where $N = \rho(\xi_p)l$ is the number of kinks and $\rho(\xi_p)$ is the linear density of kinks (number of kinks per unit

length) associated with the plastic strain, ξ_p. The surface energy is, therefore, $E_s = E_{kink}/A$ where A is the area associated with the two surfaces of one kink. A is defined as $A = 2A_0/\sin\alpha$ where α is the angle between the boundary of the fibre and the fibre axis. Thus the surface energy is given by the following equation [2, 42]

$$E_s = \frac{\sigma_{yield}\xi_p \sin\alpha}{2\rho(\xi_p)} = \frac{\sigma_{yield}(\xi_{total} - \xi_{yield})\sin\alpha}{2\rho(\xi_p)}. \quad (1)$$

We assume that the stress to initiate kinks, σ_{yield}, is similar for uncross-linked and cross-linked fibres and is 0.26 GPa, as obtained by recoil testing of PPTA-co-5XTA [22]. The total strain imposed by the shrinkage of the nylon matrix, ξ_{total}, is 3% and the critical strain to kink formation, ξ_{yield}, is 0.55% and 1% for PPXTA heat treated at 260 and 435 °C, respectively. The linear density of kinks and kink bundles, $\rho(\xi_p)$, is 16 kinks mm^{-1} and 13 bundles mm^{-1} for the fibres heat treated at 260 °C and 2 kinks mm^{-1} for the fibre heat treated at 435 °C. We may assume that one kink bundle contains five kinks. From the dark-field images, the angle, α, is 55°–65°, with an average of 60°. These data give an effective surface energy, E_s, of 34 J m^{-2} for the fibres heat treated at 260 °C and 1130 J m^{-2} for the fibre heat treated at 435 °C.

Within the above assumptions, we find that 33 times more surface energy is required to form a kink band in the cross-linked fibres heat treated at 435 °C for 1 min than in the uncross-linked fibre heat treated at 260 °C for 1 min. In the highly cross-linked fibre heat treated at 435 °C for 2 min, the energy to rupture the material is apparently lower than the energy to form kinks, thus brittle rupture predominates.

Our values of kink surface energy (30–1000 J m^{-2}) are much smaller than the 70 kJ m^{-2} obtained by Martin [1] for heat-treated PBZO. This apparent discrepancy cannot be explained only by the difference in method of kink visualization. Had we used optical microscopy we would have seen in the uncross-linked PPXTA a density of kinks, actually bundles, of 13 per mm giving a surface energy of 213 J m^{-2} instead of 34, still much lower than 70 kJ m^{-2}. Martin found a lower strain to kink formation for PBZO (0.001) than for Kevlar 49 (0.005). In contrast, the density of kinks at a given strain was larger for PBZO than for Kevlar 49. One possible explanation for the higher kink energy in the rigid-rod PBZO than in the extended-chain PPTA or PPXTA is that kinking in PBZO involves bending of covalent bonds, whereas kinking in PPTA and PPXTA can be accommodated by rotations of the amide group.

These estimated values of kink surface energy are much larger than surface energies of typical solids. For copper, the energy of formation for a grain boundary is 0.55 J m^{-2} and for an external surface is 1.43 J m^{-2} [43]. Our results show than "kinking" makes it possible for the fibres to dissipate a great amount of energy. This energy is released during the formation of the boundaries and therefore during bending of the molecules, and during local shear within the kink bands. However, the energy consumed by the fibres is not solely dissipated in kink band formation. The formation of cracks within the kink bands of uncross-linked PPXTA are equivalent to the creation of surfaces, and thus consume energy. Bulges observed on the fibre surface require void formation within the fibre and also consume energy. Finally, material rupture seen in the cross-linked fibres also consumes energy.

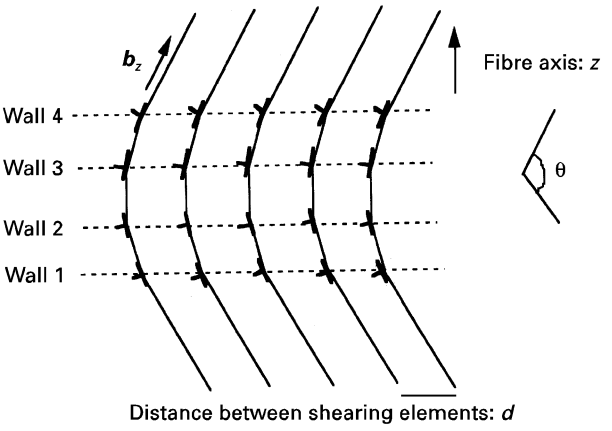

Figure 8 Schematic drawing of the dislocation model for the boundary of a kink band developed by Vladimirov *et al.* [9].

To determine what microstructural features are responsible for the increase in kink energy with cross-linking, we analysed the model developed by Vladimirov *et al.* [9]. The model assumes that the kink bands are formed primarily by microfibril slip as a result of the microfibrils being weakly connected to one another. Slip of fibrils past one another leads to the accumulation of dislocations at the kink boundary where the molecules bend. The structural model of the boundary consists of walls of edge dislocations of Burgers vector parallel to the chain axis, with an inter-dislocation distance, d, within the walls of the order of the transverse size of microfibrils, see Fig. 8. Each wall represents a small-angle boundary. The finite width, L, of the boundary results from a competition between two contributions to the specific energy: the elastic energy, W^z, associated with bending strains of the fibrils, which decreases for smoother bending (larger L), and the elastic energy, W^x, associated with the tensile strains of the fibrils which arises as the boundary expands (larger L). W^x prevents the small-angle boundaries from dispersing. As pointed out by the authors, the presence of cracks or interfibrillar stratification is not taken into account in the calculation. Microcracks would decrease W^x and result in a wider boundary than predicted by the model.

The parameters of the model are the five stiffness constants $C_{11}, C_{33}, C_{44}, C_{13}, C_{66}$ or the five moduli $E_{33}, E_{11}, K_{12}, G_{13}, G_{12}$ characteristic of the elastic deformation behaviour of a transversely isotropic material of longitudinal axis 3, the angle of the kink, θ, the Burgers vector, $\boldsymbol{b}_z$, and the size, d, of the bending or shearing elements assumed to be microfibrils. These

TABLE I

		E_{33} (GPa)	E_{11} (GPa)	K_1 (GPa)	G_{13} (GPa)	G_{12} (GPa)	Energy density, W (kJ m^{-2})	Width, L (nm)
PPTA	$d = 10$ nm	339	18	11	1	8	0.6	82
	$d = 30$ nm	339	18	11	1	8	5	650
PPDXTA	Uncross-linked	252	19	15	4	11	1.2	93
	Cross-linked	190	67	40	9	30	1.4	36

parameters make it possible to calculate the equilibrium distances between neighbouring walls or small-angle boundaries, which in turn makes it feasible to determine both the total width, L, of the boundary of the kink band and its specific energy, W. From θ, $\boldsymbol{b}_z$, and d, one can calculate the number of dislocation walls, n, and various angles, ψ_i and ϕ_i, characterizing each wall i as well as the thickness of the fibrils δ_i at each wall. Thus the structure of the boundary is defined. Using, in addition, the five stiffness constants $C_{11}, C_{33}, C_{44}, C_{13}, C_{66}$ and using the constants B_l, F_l, E_l, a_l with $l = 1, 2, 3$ defined from the stiffness constants [44], the complete system of $n-1$ equilibrium equations [9] makes it possible to solve for the equilibrium distances z_{ij} between walls i and j and therefore for the equilibrium distances between neighbouring walls z_i because $z_{ij} = \sum_{k=i}^{k=j-1} z_k$. Then the total width of the kink boundary $L = \sum_{i=1}^{n-1} z_i$ and its specific energy $W = W^x + W^z$ can be calculated.

The structure of the boundary defined by n, ψ_i, ϕ_i, and δ_i is calculated using the following equations

$$\psi_1 = \theta/2 \tag{2}$$

$$\delta_0 = d\cos(\psi_1) \tag{3}$$

$$\varphi_i = \psi_i - \sin^{-1}\left(\sin(\psi_i) - b_z\cos\left(\frac{\psi_1}{\delta_{i-1}}\right)\right) \tag{4}$$

$$\delta_i = \delta_{i-1}\frac{\cos(\psi_i - \varphi_i)}{\cos(\psi_i)} \tag{5}$$

and

$$\psi_i = \psi_1 - \left(\sum_{k=1}^{k=i-1}\varphi_k\right) \tag{6}$$

with i increasing from 1–n. n is defined as $n = i$ when $\sum_{k=1}^{k=i}\varphi_k$ reaches θ.

The complete system of $n-1$ equations which makes it possible to calculate each distance, z_{ij}, and therefore z_i from $i = 1$ to $n-1$ is

$$w_i - w_{i-1} + \sum_{j=1}^{i-1} f(z_{ji}) - \sum_{j=i+1}^{n} f(z_{ij}) = 0, \qquad i = 1, \ldots, (n-1) \tag{7}$$

with

$$w_i = \frac{E_{11}}{2}\left(1 - \frac{\delta_i}{\delta_0}\right)^2 \tag{8}$$

and

$$f(z_{ji}) = \frac{4\pi C_{44}}{C_{11}C_{66}}\frac{b_z}{d}\sum_{l=1}^{l=3}\left(\frac{B_l}{a_l} - F_l\right) \times\left(\exp\left(\frac{2\pi z_{ji}}{a_l^{1/2}d}\right) - 1\right)^{-1} \tag{9}$$

Then the specific energy, W, of the kink boundary is

$$W = W^x + W^z = \frac{1}{2}E_{11}\sum_{i=1}^{n-1} z_i\left(1 - \frac{\delta_i}{\delta_0}\right)^2 + nW_s + \sum_{i=1}^{n-1}\sum_{j=i+1}^{n} W_{int}(z_{ij}) \tag{10}$$

with

$$W_{int}(z) = \frac{2C_{44}}{C_{11}C_{66}}\frac{b_z^2}{d}\sum_{l=1}^{3} \times\left\{\left(\frac{B_l}{a_l} - F_l\right)a_l^{1/2}\ln\left[\exp\left(\frac{2\pi z}{a_l^{1/2}d}\right) - 1\right]\right\} \tag{11}$$

and

$$W_s = \frac{1}{2}W_{int}\left(z = \frac{b_z}{4}\right) \tag{12}$$

To analyse the model, the constants $E_{33}, E_{11}, K_{12}, G_{13}, G_{12}$ as well as the size, d, of the microfibrils or of the bending elements, were varied. The results are presented in Table I. The Burgers vector, $\boldsymbol{b}_z$, was chosen as 1.3 nm, the size of the repeat unit along the chain axis, and the misorientation angle, θ, was 120°. Unless otherwise indicated, the width of the bending elements, d, was taken to be 10 nm. As shown in the table, raising the size d of the bending elements for PPTA from 10 nm to 30 nm results in a dramatic increase in both the specific energy, W, of the boundary, and its width, L. However, cross-linking PPDXTA by modifying its elastic constants does not much affect the energy, and decreases the expected width of the boundary.

According to the model, the width and energy of the kink boundary depends strongly on the distance between the neighbouring planes of interslipping macromolecules. From this model it is clear that the experimentally observed increase in the specific energy of a kink with cross-linking necessitates an enlargement of the bending elements. Our hypothesis is that one mechanism by which the cross-links raise the energy to kink formation is the change of the bending elements from single molecules or small bundles of

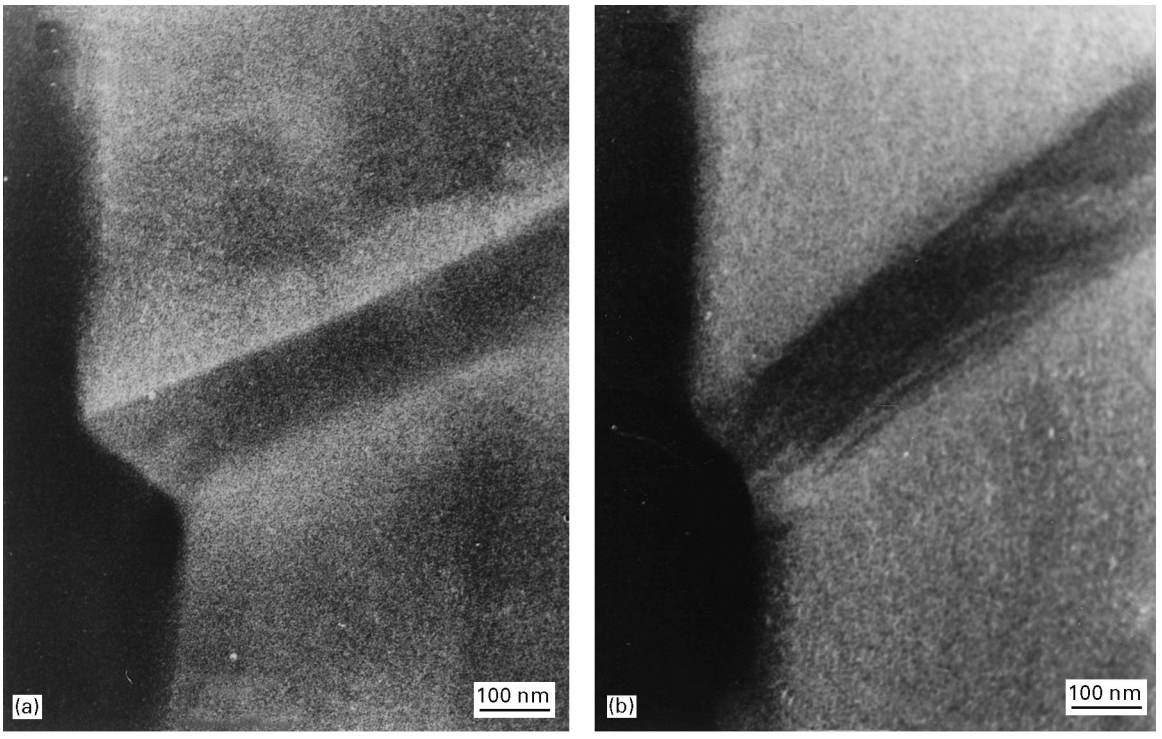

Figure 9 Equatorial dark-field TEM images of kink bands in PPXTA heat treated at (a) 260 °C for 30 s and (b) 440 °C for 30 s.

molecules to crosslinked microfibrils. If this is true, we should observe an increase in the width of the boundary predicted by the model for larger bending elements.

Fig. 9 presents equatorial dark-field images of individual kink bands in PPXTA heat treated at 260 °C for 30 s (uncross-linked) and at 440 °C for 30 s (cross-linked). The bright areas represent crystallites that scatter electrons into the objective aperture, and therefore that have good lateral packing and are oriented parallel to the fibre axis. The change in contrast at the upper tensile boundary is sharp for the uncross-linked fibres heat treated at 260 °C and more diffuse for the fibres heat treated at 440 °C. Because the contrast in these images is related to the local molecular orientation, this means that the width of the boundary is indeed wider for the fibres heat treated at 440 °C, as predicted by the Vladimirov model for larger bending elements. In the dark-field images of Fig. 9, the width of the kink boundaries on the compressive region of the kink bands is estimated to be of the order of 15 nm for PPXTA heat treated at 260 °C and 40 nm for PPXTA heat treated at 440 °C. Similarly, the width of the kink boundaries on the tensile region is estimated to be 5 nm for PPXTA heat treated at 260 °C and 20 nm for PPXTA heat treated at 410 °C. It also appears that the kink band is less uniform for the fibres heat treated at 440 °C, as indicated by the white areas. This is consistent with the shear being "blocky" or non-homogeneous in fibres heat treated at 440 °C. These observations are summarized in the schematic drawing of Fig. 10. It should be noticed that the kinks of the fibres heat treated at 260 °C were small enough for them not to contain any cracks. As mentioned earlier, the presence of cracks would have resulted in a wider boundary than predicted by the model.

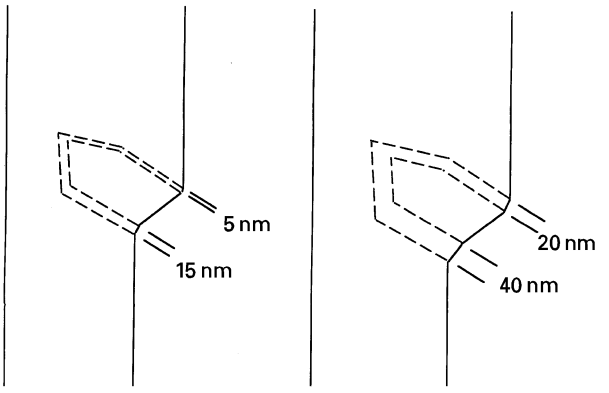

Figure 10 Schematic diagram of the change in PPXTA kink morphology observed upon heat treatment at 440 °C for 30 s. The boundaries of the kink increase in width and the heterogeneity of strain within the kink increases.

To summarize, our results suggest that one of the factors leading to improved compressive behaviour upon cross-linking is an increase in the size of the bending or shearing elements. Thus cross-linking prevents fine intermolecular shear but still allows coarse interfibrillar shear, see the schematic drawing in Fig. 11. It should be noted that kinking is not necessarily an undesirable characteristic, because it does provide toughness by absorbing a large amount of energy. By changing the heat-treatment of PPXTA fibres and therefore by varying the cross-link density, one should be able to obtain an optimum combination of compressive strength and toughness. For that, the critical strain to materials rupture should be higher than the critical strain to kink formation. Thus the formation of the cross-links would raise the energy to kink formation yet still allow the failure to proceed

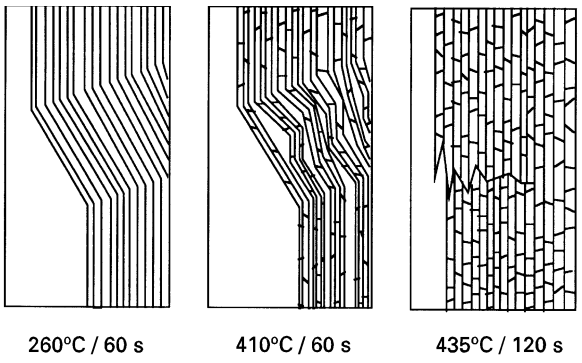

Figure 11 Schematic drawing of kink band morphology in uncross-linked PPXTA, in cross-linked PPXTA when the heat treatment is such that yielding still occurs by kinking, and a failure zone in highly cross-linked and degraded PPXTA.

by kinking without causing fracture once the deformation zone is created.

The modification of the kinking behaviour introduced by intermolecular cross-links has important implications for the fundamental mechanisms of kink formation in oriented extended-chain polymers, as well as on the nature of the microfibrillar network. The cross-links are an additional variable compared to the usual extended-chain fibres and provide a unique opportunity to test various hypotheses that have been formed in the past.

Numerous authors have concluded that the mechanism of compressive deformation is the buckling of interacting or non-interacting fibrils [5, 9, 45]. The interactions between the fibrils are typically thought to be weaker than those between molecules, because any separation above the nanometre range will render secondary bonds ineffective. The buckling theories that have been developed hold the fibrillar structure as primarily responsible for the low compressive strength, and neglect the importance of the molecular structure and of the interaction between the molecular chains. We believe that whether the initial instability results from buckling of fibrils or molecules, or from interfibrillar or intermolecular shear, the propagation step necessitates cooperative bending of the molecules at the boundary, as well as cooperative uniform or non-uniform shear between the molecules. Thus, both the microfibrillar network and the molecular structure are of importance to the compressive behaviour, as demonstrated with the PPXTA system.

As shown here with PPXTA, the compressive behaviour can be modified and kinking can be suppressed without eliminating the fibrillar structure, only by increasing the lateral interactions between molecules. Elsewhere we have shown that the torsional and transverse modulus of PPXTA is not much modified by the formation of cross-links [19]. This suggests that the cross-links predominantly form within the microfibrils, and that the shear is in part, accommodated by the interfibrillar shear. DeTeresa *et al.*'s buckling model [33] which states that the compressive strength is proportional to the lowest longitudinal shear modulus, e.g. the torsional modulus for PPXTA, is not adequate for the PPXTA system. The buckling instability is not a primary factor in the compressive behaviour of cross-linkable PPXTA, because the dramatic change in compressive behaviour is not accompanied by concomitant increase in the shear modulus. We have also shown that the uncross-linked and cross-linked PPXTA fibres display different large strain-deformation behaviour during lateral compression [19]. Whereas the uncross-linked PPXTA as well Kevlar fibres yield and plastically deform, the cross-linked PPXTA fibres exhibit a large strain elastic behaviour. Thus, shear yielding during lateral compression is significantly delayed for the cross-linked system. The higher yield stress in shear is another factor leading to improved compressive behaviour upon cross-linking. A concomitant increase in yield stress during lateral shear and kink energy in the cross-linked fibres suggest that intermolecular shear is a necessary step during the development of kink bands.

This work has made it possible to explore the role of the microfibrillar network on the compressive deformation of oriented polymers. We contend that very little differentiates an interfibrillar boundary and an intermolecular boundary except, for example, for intermolecular cross-links when available. An interfibrillar space could be defined as a region of uncross-linked material. Thus increasing the size of the microfibrils or reducing the extent of lateral density fluctuations to improve the compressive behaviour would be important only in a cross-linked system, where uncross-linked and cross-linked boundaries are clearly different. Because of molecular and fibrillar movements during heat treatment, it is possible that some cross-links form between the microfibrils and that the fibrillar structure of the heat-treated material is different from the fibrillar structure of the as-spun fibres.

The brittle rupture that takes place during axial compression prevents us from drawing conclusions on how high the strain and the energy to kink formation could get in a cross-linked, non-degraded system. In addition, the beam bending test is already used to its maximum strain potential, roughly 1.4%. For PPXTA heat treated at 440 °C for 120 s, the one or two failure zones resulting from the 1.4% strain were assumed to be kinks but could have been the result of brittle fracture as well. Nevertheless, it is possible that the microfibrillar network may limit what can be achieved in cross-linkable lyotropic systems where density fluctuations are inevitable. One possible approach might be to generate larger microfibrils or cross-linked shearing elements by optimizing the coagulation step of the spinning process. Another approach would be to increase the lateral interactions between the microfibrils and cross-link between the microfibrils. This could be done by heat treating the fibres under pressure in order to force the microfibrils close enough for the cross-linking reaction to take place, or by infiltrating the interfibrillar space with cross-linkable monomers [22]. Finally, work is being done on cross-linkable thermotropic liquid crystal polymers including XTA-equipped aromatic polyesters such as

HBA/HNA [46]. Because thermotropic polymers are processed directly from the melt, it should be possible to limit the extent of lateral density fluctuations. However, like lyotropic polymers, thermotropic polymers also possess a microfibrillar network as shown by the presence of an equatorial small-angle X-ray scattering streak, indicative of density fluctuation. By cross-linking the system before cooling, it might be possible to suppress or reduce the formation of this microfibrillar network.

4. Conclusion

A transition in compressive failure mechanism has been observed for cross-linkable PPXTA as a function of heat treatment. As-spun fibres and fibres heat treated at 260 °C fail by the formation of kinks. In contrast, fibres heat treated at 435 °C for 2 min fail by brittle fracture. The morphology of the failure areas observed with SEM suggests that the local failure mechanism involves some rupture of the fibrils and molecules. In addition, no sign of yielding preceding the fracture is displayed. Such a transition in behaviour is not observed for neat PPTA (Kevlar 49) which fails by kink formation regardless of the heat-treatment conditions.

The formation of cross-links in PPXTA fibres not only raises the strain to kink formation values but also decreases the density of kinks obtained at a given strain. The surface energy of kink bands was estimated at 34 J m^{-2} for uncross-linked PPXTA heat treated at 260 °C for 1 min, and 1126 J m^{-2} for cross-linked PPXTA heat treated at 435 °C for 1 min. Further cross-linking during a heat treatment at 435 °C for 2 min results in a transition in failure mechanism to brittle material rupture. It is possible that brittle rupture results, in part, from thermal degradation and that the kink energy would be raised further in a cross-linked, yet non-degraded material.

By changing the heat treatment of PPXTA fibres and therefore by varying the cross-link density, one should be able to obtain an optimum combination of compressive strength and toughness. Thus, the cross-links would raise the energy to kink formation yet still allow the deformation to proceed by kinking without causing fracture once the deformation zone is created.

The analysis of Vladimirov *et al.*'s [9] together with our experimental results suggest that one mechanism by which the formation of cross-links raise the energy to kink formation is the change of the bending elements from single molecules or small bundles of molecules, to cross-linked microfibrils. Thus the lateral density fluctuations from the microfibrillar network are critical to the compressive behaviour of cross-linked fibres, where an interfibrillar boundary could be defined as a region of uncross-linked material.

Our results with the cross-linkable PPXTA system demonstrate that the molecular structure is of importance to the compressive behaviour. With PPXTA, the energy to kink formation is raised not by eliminating the fibrillar structure but by increasing the lateral interactions between molecules.

Acknowledgements

This research was supported by the US Army Advanced Concept Technology Committee (DAAK6-92-K-0005). Generous support was also provided from DuPont, Hoechst-Celanese, and the NSF National Young Investigator Program (NSF-DMR-9257560).

References

1. D. C. MARTIN, PhD dissertation, The University of Massachusetts, Amherst, MA (1990).
2. D. C. MARTIN and E. L. THOMAS, *J. Mater. Sci.* **26** (1991) 5171.
3. V. V. KOZEY, H. JIANG, V. R. MEHTA and S. KUMAR, *J. Mater. Res.* **10** (1995) 1044.
4. S. J. DETERESA, S. R. ALLEN and R. J. FARRIS, in "Composite Applications: The Role of Matrix, Fiber, and Interface", edited by Tyrone Vigo and Barbara Kinzig (VCH, New York, NY 1992) Ch. 4.
5. D. L. VEZIE, PhD dissertation, Massachusetts Institute of Technology, Cambridge, MA (1993).
6. S. J. DETERESA, R. S. PORTER and R. J. FARRIS, *J. Mater. Sci.* **23** (1988) 1886.
7. A. M. KOSEVICH and V. S. BOIKO, *Usp. Fiz. Nauk* **104** (1971) 201.
8. C. Y.-C. LEE and U. SANTOSH, *Polym. Eng. Sci.* **33** (1993) 907.
9. V. I. VLADIMIROV, A. G. ZEMBIL'GOTOV and N. A. PERTSEV, *Fiz. Tverd. Tela* (*Leningrad*) **31** (1989) 233.
10. J. B. HESS and C. S. BARRETT, *Metals Trans.* **185** (1949) 599.
11. J. J. GILMAN and T. A. READ, *J. Metals* **5**(1) (1953) 49.
12. A. S. ARGON, in "Treatise on Materials Science and Technology" (Academic Press, New York, London, 1072) p. 79.
13. A. G. EVANS and W. F. ADLER, *Acta Metall.* **26** (1978) 725.
14. N. A. PERTSEV, A. E. ROMANOV and V. I. VLADIMIROV, *J. Mater. Sci.* **16** (1981) 2084.
15. N. A. PERTSEV and V. L. VLADIMIROV, *J. Mater. Sci. Lett.* **1** (1982) 153.
16. N. A. PERTSEV and A. E. ROMANOV, *Mekh. Kompoz. Mater.* **5** (1983) 781.
17. N. A. PERTSEV, V. A. MARIKHIN, L. P. MYASNIKOVA and Z. PELZBAUER, *Polym. Sci. USSR* **27** (1985) 1611.
18. N. A. PERTSEV, *Progr. Coll. Polym. Sci.* **92** (1993) 52.
19. M.-C. G. JONES, PhD dissertation, University of Michigan, Ann Arbor, MI (1995).
20. L. J. MARKOSKI, K. A. WALKER, G. A. DEETER, G. E. SPILMAN, D. C. MARTIN and J. S. MOORE, *Chem. Mater.* **5** (1993) 248.
21. G. E. SPILMAN, L. J. MARKOSKI, K. A. WALKER, G. A. DEETER, D. C. MARTIN and J. S. MOORE, *Polym. Mater. Sci. Eng.* **68** (1993) 139.
22. T. JIANG, J. RIGNEY, M.-C. G. JONES, L. J. MARKOSKI, G. E. SPILMAN, D. F. MIELEWSKI and D. C. MARTIN, *Macromolecules* **28** (1995) 3301.
23. M.-C. G. JONES, T. JIANG and D. C. MARTIN, *ibid.* **27** (1994) 6507.
24. W. WANG, W. RULAND and Y. COHEN, *Acta Polym.* **44** (1993) 273.
25. Y. COHEN, H. H. FROST and E. L. THOMAS, in "Reversible Polymeric Gels and Related Systems", edited by P. S. Russo (American Chemical Society Symposium Series, Washington, DC 1987).
26. L. FRYDMAN, University of Illinois at Chicago, unpublished research (1994).
27. T. JIANG, University of Michigan, unpublished research (1994).
28. M. J. MARKS, *Polym. Preprints* **66** (1992) 362.
29. M. J. MARKS, J. S. ERSKINE and D. A. MCCRERY, *Macromolecules* **27** (1994) 4114.
30. D. F. MIELEWSKI, D. C. MARTIN and D. R. BAUER, *Polym. Mater. Sci. Eng.* August **71** (1994) 160–61.
31. S. J. DETERESA, R. J. FARRIS and R. S. PORTER, *Polym. Compos.* **3**(2) (1982) 57.

32. D. L. VEZIE, E. L. THOMAS and W. W. ADAMS, *Polymer* **36** (1995) 1761.
33. D. C. MARTIN and E. L. THOMAS, *ibid.* **36** (1995) 1743.
34. S. J. DETERESA, S. R. ALLEN, R. J. FARRIS and R. S. PORTER, *J. Mater. Sci.* **19** (1984) 57.
35. S. L. MAYO, B. D. OLAFSON and W. A. GODDARD, *J. Phys. Chem.* **94** (1990) 8897.
36. G. E. SPILMAN, T. JIANG, J. S. MOORE and D. C. MARTIN, *Polym. Preprints* August (1994).
37. M. G. DOBB, D. J. JOHNSON and B. P. SAVILLE, *Polymer* **22** (1981) 960.
38. C. C. CHAU, J. BLACKSON and I. IM, *ibid.* **36** (1995) 2511.
39. J. P. PENNING, H. E. PRAS and A. J. PENNINGS, *Coll. Polym. Sci.* **272** (1994) 664.
40. R. J. YOUNG and P. P. ANG, *Polymer* **33** (1992) 975.
41. C. VLATTAS and C. GALIOTIS, *ibid.* **32** (1991) 1788.
42. D. C. MARTIN and E. L. THOMAS, in "Micromechanisms of Kinking in Rigid-Rod Polymer Fibers", Churchill Conference Preprints, 8th International Conference on Deformation, Yield, and Fracture of Polymers, Churchill College, Cambridge, UK (Plastics and Rubber Institute, London, UK, 1991).
43. A. L. RUOFF, "Materials Science" (Prentice-Hall, Englewood Cliffs, NJ, 1973).
44. N. A. PERTSEV, V. I. VLADIMIROV and A. G. ZEMBIL'GOTOV, *Polymer* **30** (1989) 265.
45. F. J. MCGARRY and J. E. MOALLI, *ibid.* **32** (1991) 1816.
46. T. JIANG, G. E. SPILMAN, D. C. MARTIN, P. T. MATHER and K. CHAFFEE, *Polym. Preprints* (1996).

Received 7 May
and accepted 3 October 1996